

# Performance evaluation of mullite ceramic membrane for oily wastewater treatment using response surface methodology based on Box-Behnken design

M. Arzani, H. R. Mahdavi, S. Azizi, T. Mohammadi\*

*School of Chemical, Petroleum and Gas Engineering, Iran University of Science and Technology (IUST), Narmak, Tehran, Iran*

## ARTICLE INFO

### Article history:

Received: January 6, 2018

Accepted: September 8, 2018

### Keywords:

Mullite

Wastewater treatment

Response surface methodology

Box-Behnken

\* Corresponding author;

E-mail: torajmohammadi@iust.ac.ir

Tel.: +98 21 77240540

Fax: +98 21 77240540

## ABSTRACT

Nowadays, oily wastewater is increasing along with the growth of various industries. So, wastewater treatment is necessary in order to protect the environment. In this study, a mullite ceramic membrane was prepared. Then, oily wastewater treatment with 200 mg L<sup>-1</sup> concentration was investigated by the response surface methodology based on Box-Behnken design (BBD) using Design-Expert 7.0.0 software. Membrane characterization was done using XRD, SEM, and porosity analysis. Based on XRD results, the major phase of the membrane was mullite. Furthermore, according to SEM image and porosity analysis, the pore size and the membrane porosity were 1.7 μm, 47 %, respectively. The experimental parameters were temperature (T, 20 - 40 °C), pressure (P, 2 - 4 bar) and cross flow velocity (CFV, 0.5-1.5 m s<sup>-1</sup>). In addition, the flux was considered as the response. The optimum conditions for achieving the maximum response were 39.62 °C of T, 3.92 bar of P, and 1.34 m s<sup>-1</sup> of CFV. The maximum permeate flux was 42.93 L m<sup>-2</sup> h<sup>-1</sup>. The rejection was investigated under different pressure from 2 to 4 bars. The maximum rejection was observed at 2 bars with the amount of 97.4 %.

## 1. Introduction

Along with the growth of cities, population growth and the expansion of industries and factories, the issue of environmental pollution has become more important. Oily and oil wastewaters are produced by many industries and their release in the environment has caused the ecology problem in the world. Membrane processes comprising microfiltration (MF), ultrafiltration (UF), nanofiltration (NF) and reverse osmosis (RO) have made significant advances in the treatment and pre-treatment of the industrial wastewaters.

In the oil industry, the reverse osmosis process is used as the main process for the treatment of oily wastewater and the processes mentioned above are in the field of pre-treatment [1].

Reverse osmosis is a process in which pressure is used to reverse the osmotic flow of water through a semipermeable membrane. This process is used for water sweetening for domestic use as well as for the treatment of industrial wastewater, especially in the oil and petrochemical industries. Due to the lack of water resources, this process has become especially important for domestic and industrial use in order to supply water [1, 2].

Maintenance of membrane surfaces to prevent fouling, and therefore frequent services require high costs. Membrane's Fouling, especially when the surface waters or industrial wastewaters contain a lot of organic materials is more problematic. These contaminations cause fouling and sometimes irreparable destruction of the membranes [3].

Given that today's oily wastewaters produced by industrial centers (e.g. the refinery) have become one of the major problems in the environment, it must be treated with appropriate methods before reuse or release in the environment. So far, for the treatment of oily wastewaters, some methods have been used that include the use of biotechnology based on biological degradation of oil wastes [4, 5] and physical methods like centrifugation using the centrifugal force, thermal treatment and electrochemical ways that cause breaking emulsions [5].

The aforementioned methods are very costly as an oily wastewater pre-treatment for use as feed in the units such as the reverse osmosis. It should be considered that the membrane process can now be introduced as a suitable method at an appropriate cost and industrial capabilities [6]. Ceramic porous materials are the materials widely used in the membrane industry due to their high chemical and mechanical resistance. The main application of ceramic membranes is for the treatment of industrial water and wastewater [2, 7].

In this regard, microfilter membranes can be used as a suitable method for the oily wastewaters pre-treatment for use in units such as the reverse osmosis which is a factor in reducing the fouling in these membranes as well as reducing the cost of this unit [8]. Ceramic membranes are produced in different shapes such as discs, tubes, multichannel tubes and hollow fibers [2, 7-9]. Furthermore, different materials such as alumina, zirconia, and kaolin are used for ceramic membranes preparation [10]. Rasouli et al. prepared mullite-alumina-zeolite and mullite-zeolite ceramic microfiltration membranes by extrusion method for the oily wastewater treatment. They also used coagulation to perform oily wastewater treatment in a hybrid process [11]. Sere et al. studied the treatment of vegetable oil refinery wastewater by alumina ceramic

membrane using response surface methodology. They investigated the effects of temperature, pressure and feed-flow rate on the microfiltration [12]. Rasouli et al. prepared mullite, mullite-alumina, mullite-alumina-zeolite and mullite-zeolite membranes as ceramic membranes in order to study oily wastewater treatment by adsorption- microfiltration as a hybrid process [13]. Also, Vasanth et al. prepared disk shape ceramic microfiltration membrane using clay by uniaxial compaction method for the oily wastewater treatment. They investigated the morphological characterization of these membranes including the average porosity, pore size, mechanical stability, chemical stability, and hydraulic permeance [14].

In this research, a cheap mullite ceramic membrane (using locally available materials) was prepared. The membrane porosity was improved by free silica of the sintered membranes using the sodium hydroxide solution. Moreover, the characteristics of the membrane were studied using XRD, SEM and porosity analysis. Moreover, the effects of temperature (T), pressure (P) and cross-flow velocity (CFV) as independent variables on MF oily wastewater treatment were observed by changing permeate flux (PF) as a response by response surface methodology based on Box-Behnken design (BBD) using Design-Expert software. Furthermore, the rejection results of the prepared membrane as a function of the pressure was studied.

## 2. Experimental

### 2.1. Material

The kaolin powders (SZWNK1, Iran China Clay industries) was used as the main material for the preparation of ceramic membrane. The kaolin powders composition is described in Table 1. Distilled water and sodium hydroxide pellets (Merck,  $M_w = 40.00 \text{ g mol}^{-1}$ ) were used for the sodium hydroxide solution preparation. Crude oil (Isfahan refinery) was used for feed preparation and kerosene (Kermanshah refinery) was used for the permeate concentration measurement using a UV-visible spectrophotometer. The chemical and physical specification of the crude oil and kerosene are shown in Table 2.

Table 1. Kaolin composition reported by the manufacturer [15]

Component name	SiO <sub>2</sub>	Al <sub>2</sub> O <sub>3</sub>	Fe <sub>2</sub> O <sub>3</sub>	TiO <sub>2</sub>	CaO	MgO	Na <sub>2</sub> O	K <sub>2</sub> O	L.O.I
Mole %	63.63	24.05	0.65	0.04	1.40	0.50	0.30	0.20	9.22

Table 2. Chemical and physical specification of the crude oil and kerosene

Property	Unit		
		Crude oil	Kerosene
Density at 15 °C	----	0.8602	0.7978
API Gravity	API	33.0	-
Kinematic Viscosity at 10 °C	mm <sup>2</sup> s <sup>-1</sup>	18.43	-
Kinematic Viscosity at 20 °C	mm <sup>2</sup> s <sup>-1</sup>	11.84	-
Kinematic Viscosity at 40 °C	mm <sup>2</sup> s <sup>-1</sup>	6.319	-

## 2.2. Membrane preparation

A mesh sieve No. 200 was used to filter the kaolin powder. Then, it was shaped into a disk with 21 mm in diameter and 1.2 mm in thickness using a uniaxial press under pressure of 500 bar for 2 min. After pressing, disk samples were placed inside a furnace (Zohouri Furnace Industries). The temperature program of the furnace was set to initially reach a temperature of 550 °C and the membranes were at this temperature for 1 h. The temperature was then increased to 950 °C and after 1 h at this temperature, it was increased to 1150 °C. The process of sintering the membrane completed within 3 h. At all stages, the temperature increase was adjusted with a constant gradient of 5 °C min<sup>-1</sup> [15, 16].

Free silica of the sintered membranes was removed using NaOH solution [15]. It was performed at the temperature, the removal time and NaOH concentration of 75 °C, 8 h, and 35 w.t %, respectively. After the free silica removal, the membranes were washed with distilled water in order to remove impurities from the membrane pores and surfaces. Then, the prepared membranes were dried.

## 2.1. Calculation

Water permeate flux for the ceramic membrane was determined from Eq. 1:

$$\text{Permeate flux} = \frac{V}{A \times t} \quad (1)$$

Where V is the volume (L) of the permeated water from the membrane. A and t are an effective area of the membrane (m<sup>2</sup>) and filtration time (h), respectively [17].

One of the important parameters of the filtration processes is the rejection percentage which is calculated from Eq. 2:

$$\text{Rejection (\%)} = \left(1 - \frac{C_p}{C_f}\right) \times 100 \quad (2)$$

C<sub>p</sub> and C<sub>f</sub> are the concentrations of impurities in the product and feed respectively [18].

## 2.2. Characterization

The membrane porosity was determined using the difference between the dry membrane weight and the membrane weight which was soaked in the pure water for 24 h. Next, porosity of the membranes was determined using the following equation:

$$\text{Porosity (\%)} = \left(\frac{W_1 - W_2}{\rho_w V_M}\right) \times 100 \quad (3)$$

W<sub>1</sub> and W<sub>2</sub> are the soaked and dry membrane's weight, respectively and V<sub>M</sub> is the volume of the membrane. Furthermore, ρ<sub>w</sub> is the water density at the experiment temperature [16].

X-ray diffraction (XRD, Philips PW1800, Cu lamp (40 kV and 30 mA)) and scanning electron microscope (SEM, Viga Tescan) were used to determine the phase structure of the membrane and analyze the structure of the membrane surface, respectively. In addition, the permeate concentration was measured using a UV–visible spectrophotometer (Shimadzu UV-1700, Kyoto, Japan) [14]. Moreover, droplets size distribution of oil emulsion was determined using the Dynamic light scattering (DLS).

The average pore size was determined using ImageJ software (version 1.4) by SEM images. For this purpose, 6 SEM images were taken randomly. Then, the average pore diameter of each membrane SEM image was determined as follows:

$$D_{ave} = \left[ \frac{\sum_{i=1}^n n_i d_i^2}{\sum_{i=1}^n n_i} \right]^{0.5} \quad (4)$$

Where  $n_i$  and  $d_i$  are the pore number and pore diameter, respectively.  $D_{ave}$  is the average pore diameter ( $\mu\text{m}$ ). Finally, the average value of 6 SEM images was reported as the membrane average pore diameter.

### 2.3. Feed

For experiments, a crude oil and water emulsion with 200 ppm oil concentration in the feed was prepared. The calculated amount of heavy oil for this concentration was added to distilled water and the powerful agitator was used to homogenize the feed water and oil at 25 °C. The low amount of crude oil in water emulsion became stabilized adequately without any other surfactant addition because of some natural surfactant presence in the crude oil [17].

### 2.4. Experimental setup and module

To perform filtration tests, the stainless steel module according to Figure 1 (a)-which consists of two parts- was used. These parts are sealed by an O-ring and the membrane is placed between the two O-rings. The filtration setup as shown in Figure 1 (b) includes a pump, a feed tank, a temperature sensor, a coolant, a pressure gauge and a flowmeter.

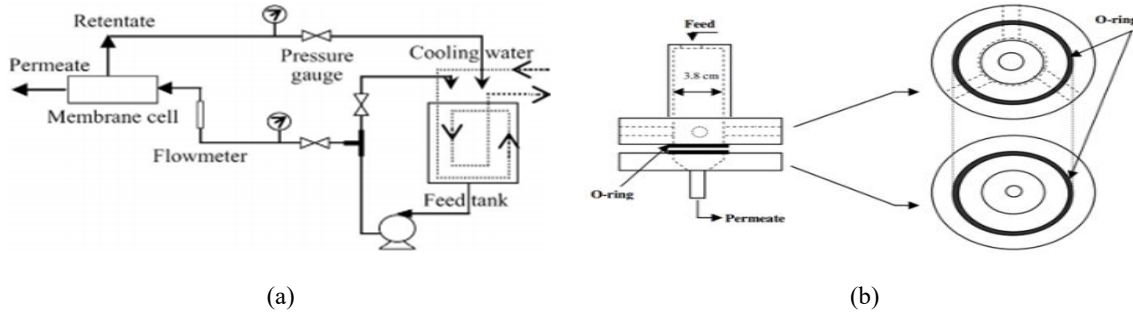


Figure 1. a) Experimental setup and b) module

## 2.5. Experimental design

The experimental design for the oily wastewater treatment was done by the response surface methodology (RSM) based on Box-Behnken design (BBD) using Design Expert 7.0.0 software. The Eq. 5 describes the quadratic polynomials for permeate flux using the encoded parameters[19].

$$\eta = \beta_0 + \sum_{j=1}^k \beta_j x_j + \sum_{j=1}^k \beta_{jj} x_j^2 + \sum_{i < j=2}^k \sum_{i=1}^k \beta_{ij} x_i x_j + \dots + e_i \quad (5)$$

In the above equation,  $\eta$  is the predicted response for permeate flux,  $x_i$  and  $x_j$  are the independent coded variables,  $\beta_0$  is the constant coefficient,  $\beta_i$  and  $\beta_j$  are linear coefficients,  $\beta_{ii}$  and  $\beta_{jj}$  are quadratic and interaction coefficients respectively and  $e_i$  is the error[19].

Table 3. Independent variables and their associated levels

Independent variable	-1	0	+1
Temperature (°C)	20	30	40
Pressure (bar)	2	3	4
Cross flow velocity (m s <sup>-1</sup> )	0.5	1	1.5

## 3. Results and discussion

### 3.1. Characterization

The prepared membrane porosity based on Eq. 3 was calculated to be 47 %. XRD analysis for the prepared membranes is presented in Figure 2. According to this Figure, the major phases are Mullite ( $\text{Al}_6\text{Si}_2\text{O}_{13}$ ) and Quartz ( $\text{SiO}_2$ ) and the minor phase is Anorthite  $(\text{Ca, Na})(\text{Si, Al})_4\text{O}_8$  for the prepared membranes. Increasing the free silica removal resulted in the membrane porosity increment [15].

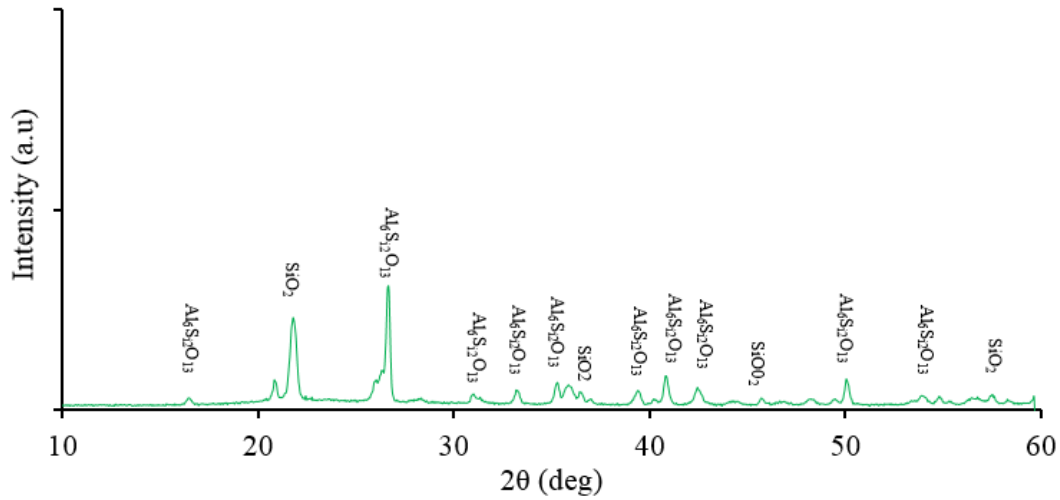


Figure 2. XRD of the prepared membrane

Figure 3 (a and b) shows SEM images of the surface and cross-section of the prepared membrane, respectively. Images show that the surface is porous and even. Furthermore, the membrane average pore diameter was 1.7  $\mu\text{m}$ .

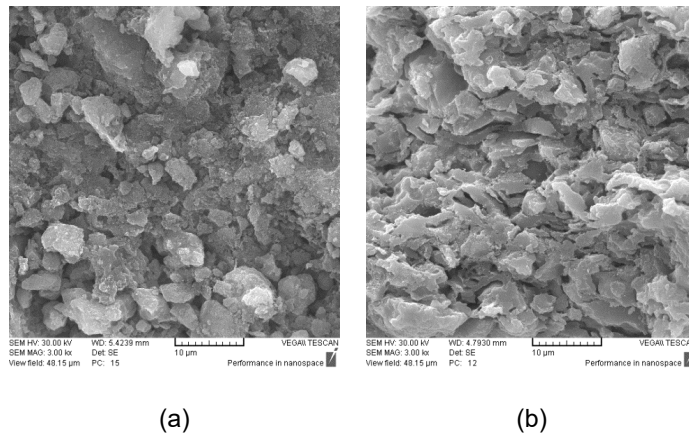


Figure 3. SEM images of prepared membranes: a) surface and c) cross section

Figure 4. shows the droplet size distributions of the oil emulsion. As observed, the average oil droplet size is 1.35  $\mu\text{m}$ .

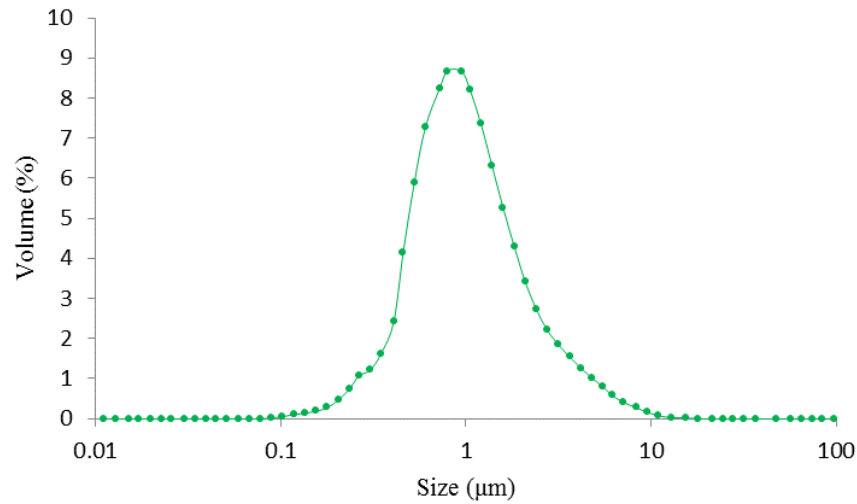


Figure 4. Droplets size distribution of oil emulsion

### 3.2. Experimental design

The experimental design of the response surface has four main steps for the optimization process: 1. Form a proper design, 2. The proposition of a statistical model based on the regression analysis method, 3. Verification of the provided model, 4. Prediction of the response variable based on the proposed model [20].

Experiments determined by the experimental design were done and equation 6 was determined using the statistical method of the response surface. This equation indicates the experimental relationship between the independent variables and the permeate flux.

$$\begin{aligned} \text{Permeate flux} = & - 10.62 - 0.24 \times T + 22.82 \times P + 1.04 \times \text{CFV} + 0.04 \times T \times P \\ & + 0.08 \times T \times \text{CFV} + 0.35 \times P \times \text{CFV} + 4.67 \times 10^{-3} \times T^2 - 2.95 \times P^2 - 1.33 \times \text{CFV}^2 \end{aligned} \quad (6)$$

The amount of permeate flux is predicted by the model and  $T$ ,  $P$ , and  $\text{CFV}$  are the independent variables of the temperature, pressure and cross-flow velocity, respectively. To verify the validity of the proposed model, analysis of variance, correlation coefficient ( $R^2$ ) and residual diagrams were investigated.

Table 4. BBD for the extraction based on the coded values

Run	T (°C)	P (bar)	CFV (m s <sup>-1</sup> )	Permeate flux (L m <sup>-2</sup> h <sup>-1</sup> )
1	40	3	1.5	38.6
2	30	4	0.5	37.1
3	40	4	1	42.9
4	30	3	1	35.6
5	20	2	1	23.3
6	20	4	1	36.4
7	20	3	1.5	33.6
8	40	2	1	28.1
9	30	3	1	34.8
10	30	4	1.5	39.5
11	30	3	1	35.1
12	20	3	0.5	32.8
13	30	2	1.5	26.3
14	40	3	0.5	36.2
15	30	2	0.5	24.6

### 3.3. Analysis of variance

The statistical method of analysis of variance examines the significance level and also significance of the entire model and its component as well. The analysis of the variance of the second order model is presented in Table 5. As seen, the p-value of the model with a 95 % confidence level is less than 0.0001 for the permeate flux,. The proposed model is meaningful because the p-value is smaller than 0.05. Also, the p-value greater than 0.05 for the non-fit of the model is an indicator for verifying the high accuracy of the model for the prediction of the estimated values for each experiment. In other words, the nonsensical fit indicates that the distance between the real and predicted values is negligible. As a general rule, the p-values less than 0.05 indicate the significance of the parameter, and on the other hand, the p-values greater than 0.1 represent the nonsignificance [21, 22]. Therefore, according to the variance analysis table, all three variables of temperature, pressure, and crossflow velocity were effective in this experiment.

The value of  $R^2 = 0.9954$  indicates the correlation between the values obtained from the experiment and the model determined, which confirms the validity of the model. Also, Adeq-Precision of 34.762, which represents the difference between the values determined by the model with the average value of the prediction error, showed that the model reports the behavior of the permeate flux well. In general, the values above 4 indicate the correctness of the model.

The predicted response and the associated experimental response are presented in Figure 5. As the data points in this graph become closer to the 45° line, the agreement between the predicted and experimental values is more appropriate. Thus, as shown, the predicted values and the experimental values

have good agreement indicating that the model has the potential to predict the response with high accuracy.

Table 5. ANOVA results of the quadratic model for permeate flu

Source	Sum of Squares	Degrees of freedom	Mean Square	F Value	P Value
Model	449.97	9	50	119.94	<0.0001
Temperature (A)	48.51	1	48.51	116.38	0.0001
Pressure (B)	359.12	1	359.12	861.54	<0.0001
Cross flow velocity (C)	6.66	1	6.66	15.98	0.0103
AB	0.72	1	0.72	1.73	0.2451
AC	0.64	1	0.64	1.54	0.2703
BC	0.12	1	0.12	0.29	0.6110
A <sup>2</sup>	0.8	1	0.8	1.93	0.2235
B <sup>2</sup>	32.31	1	32.31	77.52	0.0003
C <sup>2</sup>	0.41	1	0.41	0.98	0.3667
Lack of fit	1.76	3	0.59	3.59	0.2256
R <sup>2</sup>			0.9954		
R <sup>2</sup> Adj			0.9871		
R <sup>2</sup> Pred			0.9362		
Adeq precision			34.762		

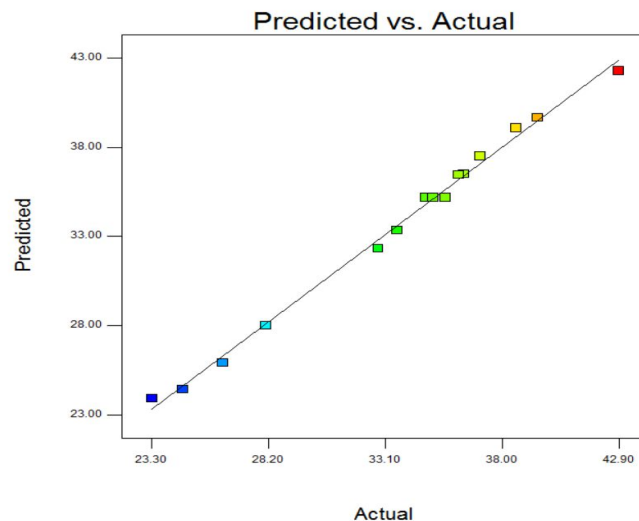
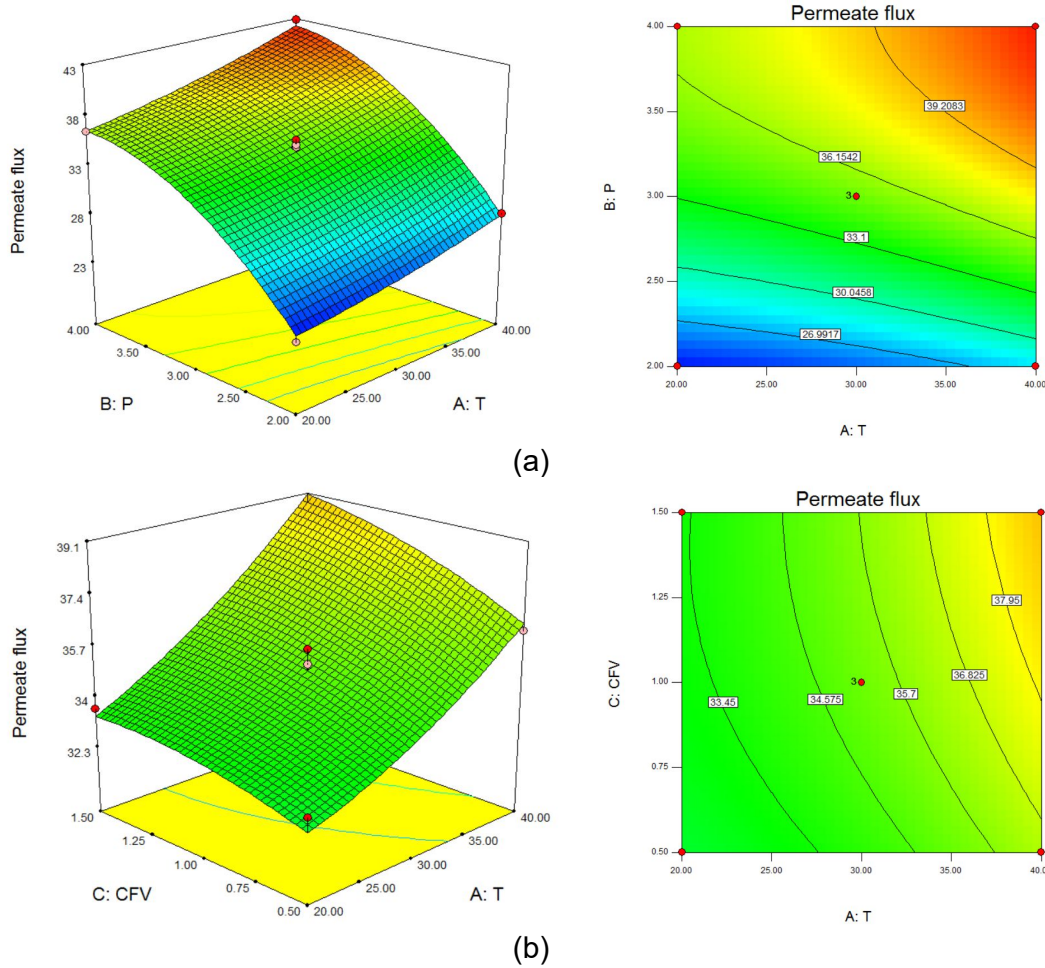


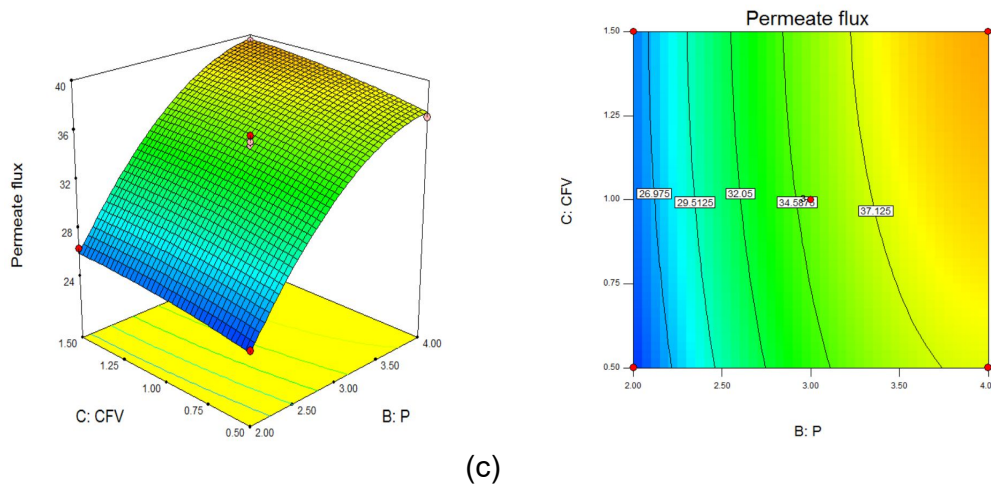
Figure 5. Predicted response versus experimental response

### 3.4. Effect of independent variables

The results of operating conditions including pressure, temperature and cross-flow velocity on the membrane performance are shown in Figure 6. Effects of the pressure were investigated in a range of 2–4 bars. Regarding Figures 6 (a) and (c), an increase in pressure will increase the permeate flux. However, at high pressures, the permeate flux is almost constant. Based on Darcy's law, increasing the pressure results in permeate flux increments whereas membrane fouling due to a compensated fouling layer formation on the membrane surface causes to permeate flux decrements [14, 23]. The effects of temperature were investigated in a range of 20–40 °C. According to Figures 6 (a) and (b), increasing the temperature enhances the permeate flux. Temperature increasing has two different effects: First, it increases the osmotic

pressure which in turn decreases the permeate flux [24, 25]. Second, it decreases viscosity significantly due to permeation which is mainly gas oil ;hence, diffusivities of solvent and solutes enhance which next increase the permeate flux [26]. Effects of cross-flow velocity were also investigated in a range of 0.5–1.5 m s<sup>-1</sup>. As shown in Figures 6 (b) and (c), by increasing the cross-flow velocity the permeate flux enhances. The cross-flow velocity enhances turbulence over the membrane surface thus mass transfer coefficient increases [26, 27].





(c)  
Figure 6. Effect of independent variables on permeate flux

### 3.4.1. Rejection

The rejection results of the prepared membrane as a function of pressure are shown in Figure 7. In order to determine the membrane rejection, different pressures of 2, 3, and 4 bar at a temperature of 25 °C and cross flow velocity of 1.5 m s<sup>-1</sup> were considered. According to Figure 7, the rejection was 97.4 % at a pressure of 2 bar. Furthermore, the membrane rejection decreases by pressure increasing. This can be due to the passing of more oil droplets through the membrane at higher pressure [27].

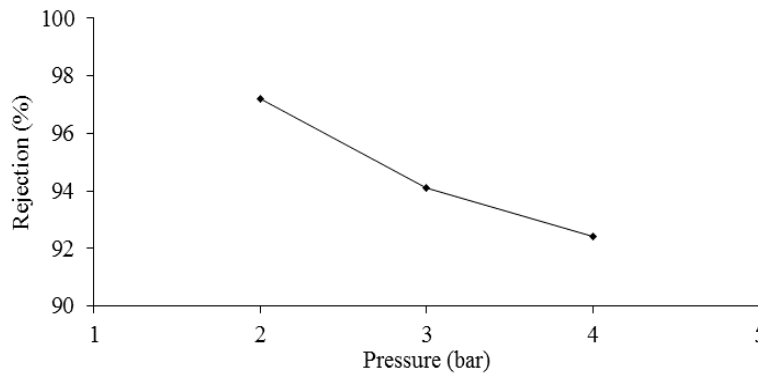


Figure 7. Rejection of the prepared membrane as a function of pressure (T= 25 °C, CFV=1.5 m s<sup>-1</sup>)

## 4. Conclusion

The prepared ceramic membrane with a porosity of 47 % and pore size of 1.7 μm under pressure of 3.92 bars, temperature of 39.62 °C and cross flow velocity of 1.34 m s<sup>-1</sup> had the highest permeate flux of 42.93 L m<sup>-2</sup> h<sup>-1</sup>. The percentage of membrane rejection for a feed of 200 mg L<sup>-1</sup> at a pressure of 2 bars was 97.4 %. To conclude, the results of the present study showed that oily wastewater can be pre-treated using the microfilter ceramic membrane and can

be used in units such as reverse osmosis in order to supply suitable quality water for various industrial uses.

### Nomenclature

P	Pressure
CFV	Cross Flow velocity
T	Temperature
PF	Permeate Flux
R	Rejection
$C_p$	Concentrations of impurities in the product
$C_f$	Concentrations of feed
Porosity	Porosity
$W_1$	Soaked membrane's weight
$W_2$	Dry membrane's weight
$\rho_w$	Water density
$V_M$	Volume of the membrane
$D_{ave}$	Membrane average pore diameter
$\eta$	Predicted response
$x_i, x_j$	Independent factors
$\beta_0$	Constant coefficient
$\beta_j$	Coefficient for linear effect
$\beta_{jj}$	Coefficient for quadratic effect
$\beta_{ij}$	Coefficient for interaction effect
$e_i$	Error

### References

- [1] S.S. Shenvi, A.M. Isloor, and A.F. Ismail, "A review on RO membrane technology: Developments and challenges." *Desalination (Supplement C)*, vol. 368, pp. 10-26, 2015.
- [2] J.Z. Hamad, C. Ha, M.D. Kennedy, G.L. Amy, "Application of ceramic membranes for seawater reverse osmosis (SWRO) pre-treatment." *Desalination and Water Treatment*, vol. 51, pp. 4881-4891, 2013.
- [3] S. Lee, C. Boo, M. Elimelech, S. Hong, "Comparison of fouling behavior in forward osmosis (FO) and reverse osmosis (RO)." *Journal of Membrane Science*, vol.365, pp. 34-39, 2010.
- [4] K. Karakulski, W.A. Morawski, and J. Grzechulska, "Purification of bilge water by hybrid ultrafiltration and photocatalytic processes." *Separation and Purification Technology*, vol. 14, pp. 163-173, 1998.
- [5] M. Cheryan, and N. Rajagopalan, "Membrane processing of oily streams. Wastewater treatment and waste reduction." *Journal of Membrane Science*, vol. 151, pp.13-28, 1998.
- [6] J. Mueller, Y. Cen, and R.H. Davis, "Crossflow microfiltration of oily water." *Journal of Membrane Science*, vol. 129, pp. 221-235, 1997.
- [7] M. Lee, Z. Wu, and K. Li—y, "Advances in ceramic membranes for water treatment, in *Advances in Membrane Technologies for Water Treatment*." *Woodhead Publishing*, Oxford. pp. 43-82, 2015.

- [8] P. Liu, and G.F. Chen, "Porous Materials: Processing and Applications." *Elsevier Science*, 2014.
- [9] F. Händle, , "Extrusion in Ceramics.", *Springer Berlin Heidelberg*, 2009.
- [10] A. Basile, A. Cassano, and N.K. Rastogi, "Advances in Membrane Technologies for Water Treatment: Materials," *Processes and Applications*. 2015: Elsevier Science.
- [11] Y. Rasouli, M. Abbasi, and S.A. Hashemifard, "Investigation of in-line coagulation-MF hybrid process for oily wastewater treatment by using novel ceramic membranes." *Journal of Cleaner Production*, vol. 161, pp. 545-559, 2017.
- [12] Z. Šereš, N. Maravić , A. Takači, I. Nikolić. "Treatment of vegetable oil refinery wastewater using alumina ceramic membrane: optimization using response surface methodology." *Journal of Cleaner Production*, vol 112, pp. 3132-3137, 2016.
- [13] Y. Rasouli, , M. Abbasi, and S.A. Hashemifard, "Oily wastewater treatment by adsorption-MF hybrid process using PAC, natural zeolite powder and low cost ceramic membranes." *Water Science and Technology*, vol.??, pp. 72, 2017.
- [14] D. Vasanth, G. Pugazhenth, and R. Uppaluri, "Performance of low cost ceramic microfiltration membranes for the treatment of oil-in-water emulsions." *Separation Science and Technology*, vol. 48, pp. 849-858, 2013.
- [15] M. Arzani, H. Mahdavi, O. bakhtiari, T. Mohammadi "Preparation of mullite ceramic microfilter membranes using Response surface methodology based on central composite design." *Ceramics International*,/ vol. 42, pp. 8155-8164, 2016.
- [16] O. Bakhtiari, M. samei , T. mohammadi and H. Taghikarimi "Preparation and characterization of mullite tubular membranes." *Desalination and Water Treatment*, vol. 36, pp. 210-218, 2011.
- [17] S.J. Lue, J. Chow, C Chien, H. Chen "Cross-Flow Microfiltration of Oily Water using a Ceramic Membrane: Flux Decline and Oil Adsorption." *Separation Science and Technology*, vol. 44, pp. 3435-3454, 2009.
- [18] M. Abbasi, T. Mohammadi and M. Mirfendereski, "Oily wastewater treatment using mullite ceramic membrane." *Desalination and Water Treatment*, vol. 37, pp. 21-30, 2012.
- [19] A. Bayat, H.R. Mahdavi, M. kazemimoghaddam and T. Mohammadi, "Preparation and characterization of  $\gamma$ -alumina ceramic ultrafiltration membranes for pretreatment of oily wastewater." *Desalination and Water Treatment*, vol. 57, pp. 24322-24332, 2016.

- [20] K. Wantala, E. Khongkasem, N. Khlongkarpanich and S. Sthiannopkao "Optimization of As (V) adsorption on Fe-RH-MCM-41-immobilized GAC using Box–Behnken Design: Effects of pH, loadings, and initial concentrations." *Applied geochemistry*, vol. 27, pp. 1027-1034, 2012.
- [21] M. Mourabet, A.E. Rhilassi, H.E. Boujaady, M.B. Ziatni, R.E. Hamri and A.Taitai, "Removal of fluoride from aqueous solution by adsorption on Apatitic tricalcium phosphate using Box–Behnken design and desirability function." *Applied Surface Science*, vol. 258, pp. 4402-4410, 2012.
- [22] Z. Zhang, Q. Pang, M. Li, H. Zheng, H. Chen and K. Chen, "Optimization of the condition for adsorption of gallic acid by *Aspergillus oryzae* mycelia using Box-Behnken design." *Environmental Science and Pollution Research*, vol. 22, pp. 1085-1094, 2015. [23] H.R. Mahdavi, M. Arzani, and T. Mohammadi, "Synthesis, characterization and performance evaluation of an optimized ceramic membrane with physical separation and photocatalytic degradation capabilities." *Ceramics International*, 2018.
- [24] T. Mohammadi, and A. Esmaeilifar, "Wastewater treatment of a vegetable oil factory by a hybrid ultrafiltration-activated carbon process." *Journal of Membrane Science*, vol. 254, pp. 129-137, 2005.
- [25] A. Salahi, et al., "Oily wastewater treatment using ultrafiltration." *Desalination and Water Treatment*, vol. 6, pp. 289-298, 2009.
- [26] M. Abbasi, A. Salahi, M. Mirfendereski, T. Mohammadi, "Dimensional analysis of permeation flux for microfiltration of oily wastewaters using mullite ceramic membranes." *Desalination*, vol. 252, pp. 113-119, 2010.
- [27] S.R.H. Abadi, M.R. Sebzari, M. Hemati, F. Rekabdar, T. Mohammadi "Ceramic membrane performance in microfiltration of oily wastewater." *Desalination*, vol. 265, pp. 222-228, 2011.

## ارزیابی عملکرد غشای سرامیکی مولایتی برای تصفیه پساب نفتی با استفاده از طراحی روش سطح پاسخ بر اساس طرح باکس بیکن

مهران ارزانی، حمید رضا مهدوی، صبا عزیزی، تورج محمدی\*

تهران، نارمک، دانشگاه علوم و تحقیقات، دانشکده مهندسی شیمی، نفت و گاز

### مشخصات مقاله

تاریخچه مقاله:

دریافت: ۱۶ دی ۱۳۹۶

پذیرش نهایی: ۱۷ شهریور ۱۳۹۷

کلمات کلیدی:

مولایت

تصفیه پساب

روش سطح پاسخ

باکس بیکن

\* عهده‌دار مکاتبات؛

رایانامه: [torajmohammadi@iust.ac.ir](mailto:torajmohammadi@iust.ac.ir)

تلفن: +۹۸ ۲۱ ۷۷۲۴۰۵۴۰

دورنگار: +۹۸ ۲۱ ۷۷۲۴۰۵۴۰

### چکیده

امروزه پساب نفتی با رشد صنایع مختلف افزایش می‌یابد. تصفیه پساب برای حفاظت از محیط زیست ضروری است. در این مطالعه غشای سرامیکی مولایتی ساخته شد و سپس تصفیه پساب نفتی با غلظت  $200 \text{ mg L}^{-1}$  با استفاده از روش تعیین سطح پاسخ و نرم افزار Design-Expert 7.0.0 مورد بررسی قرار گرفت. ارزیابی ساختاری غشا با استفاده از آنالیز XRD، SEM و تخلخل سنجی انجام شد. نتایج نشان داد بیشینه فاز مولایت، اندازه حفره  $1/7 \mu\text{m}$  و تخلخل % ۴۷ است. پارامترهای آزمایش عبارت‌اند از دما ( $^{\circ}\text{C}$ ) ۴۰-۲۰، فشار (bar) ۴-۲ و سرعت جریان عرضی ( $\text{m s}^{-1}$ ) ۰/۵-۱/۵. شار به عنوان پاسخ در نظر گرفته شد. شرایط بهینه برای دستیابی به بیشینه پاسخ در دمای  $39/62^{\circ}\text{C}$ ، فشار  $3/98 \text{ bar}$  و سرعت جریان عرضی  $1/43 \text{ m s}^{-1}$  شد. حداکثر تراوش غشا برابر  $L$  تا  $4 \text{ m}^2 \text{ h}^{-1}$  بود. ضریب پس‌دهی در فشارهای مختلف از  $2 \text{ bar}$  تا  $4 \text{ bar}$  مورد بررسی قرار گرفت. بیشینه ضریب پس‌دهی در فشار  $2 \text{ bar}$  برابر  $97/4\%$  شد.